

High hole mobility p-type GaN with low residual hydrogen concentration prepared by pulsed sputtering

Cite as: APL Mater. 4, 086103 (2016); <https://doi.org/10.1063/1.4960485>

Submitted: 22 June 2016 • Accepted: 25 July 2016 • Published Online: 05 August 2016

Yasuaki Arakawa, Kohei Ueno, Atsushi Kobayashi, et al.



View Online



Export Citation



CrossMark

ARTICLES YOU MAY BE INTERESTED IN

[Electrical properties of Si-doped GaN prepared using pulsed sputtering](#)

Applied Physics Letters **110**, 042103 (2017); <https://doi.org/10.1063/1.4975056>

[Electron transport properties of degenerate n-type GaN prepared by pulsed sputtering](#)

APL Materials **5**, 126102 (2017); <https://doi.org/10.1063/1.5008913>

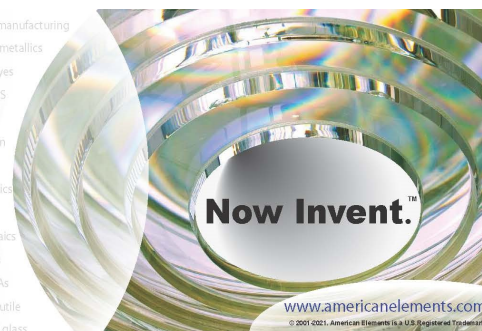
[Heavy doping effects in Mg-doped GaN](#)

Journal of Applied Physics **87**, 1832 (2000); <https://doi.org/10.1063/1.372098>



yttrium iron garnet glassy carbon beamsplitters fused quartz additive manufacturing
 zeolites III-IV semiconductors gallium lump copper nanoparticles organometallics
 nano ribbons barium fluoride europium phosphors photonics infrared dyes
 epitaxial crystal growth ultra high purity materials transparent ceramics CIGS
 cerium oxide polishing powder surface functionalized nanoparticles MRE grade materials thin film
 silver nanoparticles perovskites beta-barium borate rare earth metals quantum dots
 osmium scintillation Ce:YAG refractory metals laser crystals
 anode lithium niobate InAs wafers dysprosium pellets MOFs AuNPs
 chalcogenides ZnS CdTe perovskite crystals transparent ceramics

The Next Generation of Material Science Catalogs



High hole mobility p-type GaN with low residual hydrogen concentration prepared by pulsed sputtering

Yasuaki Arakawa,¹ Kohei Ueno,¹ Atsushi Kobayashi,¹ Jitsuo Ohta,^{1,2} and Hiroshi Fujioka^{1,3}

¹*Institute of Industrial Science, The University of Tokyo, 4-6-1 Komaba, Meguro, Tokyo 153-8505, Japan*

²*PRESTO, Japan Science and Technology Agency (JST), 4-1-8 Honcho, Kawaguchi, Saitama 332-0012, Japan*

³*ACCEL, Japan Science and Technology Agency (JST), 5 Sanbancho, Chiyoda-ku, Tokyo 102-0075, Japan*

(Received 22 June 2016; accepted 25 July 2016; published online 5 August 2016)

We have grown Mg-doped GaN films with low residual hydrogen concentration using a low-temperature pulsed sputtering deposition (PSD) process. The growth system is inherently hydrogen-free, allowing us to obtain high-purity Mg-doped GaN films with residual hydrogen concentrations below $5 \times 10^{16} \text{ cm}^{-3}$, which is the detection limit of secondary ion mass spectroscopy. In the Mg profile, no memory effect or serious dopant diffusion was detected. The as-deposited Mg-doped GaN films showed clear p-type conductivity at room temperature (RT) without thermal activation. The GaN film doped with a low concentration of Mg ($7.9 \times 10^{17} \text{ cm}^{-3}$) deposited by PSD showed hole mobilities of 34 and $62 \text{ cm}^2 \text{ V}^{-1} \text{ s}^{-1}$ at RT and 175 K, respectively, which are as high as those of films grown by a state-of-the-art metal-organic chemical vapor deposition apparatus. These results indicate that PSD is a powerful tool for the fabrication of GaN-based vertical power devices. © 2016 Author(s). All article content, except where otherwise noted, is licensed under a Creative Commons Attribution (CC BY) license (<http://creativecommons.org/licenses/by/4.0/>). [<http://dx.doi.org/10.1063/1.4960485>]

GaN has attracted considerable attention as a material for power devices because of its high breakdown voltage, high mobility, and high thermal stability. Despite these excellent properties, the performances of GaN-based vertical power devices remain insufficient due to the lack of high-quality GaN bulk substrates and an immature epitaxial growth process. With recent progress in the preparation processes of GaN bulk substrates for the development of vertical power devices, many research groups have attempted to improve the electrical and structural properties of homoepitaxially grown GaN, mainly by reducing residual impurities and employing doping.^{1,2} The fabrication of vertical devices such as p-n junction diodes^{3,4} and trench metal-oxide semiconductor field-effect transistors⁵ requires the precise control of the p-type dopant in GaN and high-quality p-type GaN. However, p-type doping via conventional metal organic chemical vapor deposition (MOCVD) results in low hole mobility due to the defects caused by doping with high concentrations (above 10^{19} cm^{-3}) of Mg and the high residual hydrogen concentration. The residual hydrogen concentration can be reduced by thermal activation;⁶ however, large quantities of hydrogen atoms with concentration higher than $1 \times 10^{18} \text{ cm}^{-3}$ often remain in the films.⁷ These hydrogen atoms can form Mg-N-H complexes in GaN and compensate Mg acceptors, deteriorating the electrical transport properties of p-type GaN. In addition, hydrogen atoms in p-type GaN may reduce the reliability of devices such as light-emitting diodes (LEDs) and lasers due to the diffusion of hydrogen atoms driven by current injection.⁸

With the goal of dramatically reducing the hydrogen concentration in p-type GaN films, we have applied a new growth technique known as pulsed sputtering deposition (PSD). PSD is an attractive method for the industrial growth of GaN due to its high productivity and scalability. Recent progress in PSD has enabled the growth of device-quality group III nitrides at much lower

temperatures compared to the conventional MOCVD process.^{9–12} Various devices including LEDs, HEMTs, and metal-insulator-semiconductor field-effect transistors (MISFETs) prepared by PSD have been successfully operated. PSD is considered as a suitable method for growing high-purity p-type GaN because the raw materials of the PSD growth system do not contain hydrogen atoms. PSD is also thought to facilitate the formation of abrupt p–n junctions, which are necessary to construct vertical power devices, and can produce p-type GaN at the low growth temperature of 480 °C.¹⁰ Moreover, n-type GaN produced using PSD shows a high electron mobility of approximately $1000 \text{ cm}^2 \text{ V}^{-1} \text{ s}^{-1}$ with a carrier concentration on the order of 10^{16} cm^{-3} . However, little has been reported on the electrical properties of p-type GaN produced via PSD.

In this study, we have demonstrated the growth of p-type GaN with low hydrogen concentration using PSD and investigated how the concentrations of Mg dopant and residual donors affect the hole transport properties.

We prepared 1- μm -thick Mg-doped GaN films with 20-nm-thick heavily Mg-doped contact layers on semi-insulating GaN templates with a growth rate of 1–2 $\mu\text{m}/\text{h}$ using PSD. The details of the growth procedure are described elsewhere.^{9–12} The Mg doping concentration of the 1- μm -thick GaN films varied from 7.9×10^{17} to $6.1 \times 10^{19} \text{ cm}^{-3}$. The Mg concentration in the top contact layer was set at $2.0 \times 10^{20} \text{ cm}^{-3}$. The concentrations of Mg dopants and residual impurities were evaluated by secondary ion mass spectroscopy (SIMS). The threading dislocation density of the GaN template was a latter half of 10^8 cm^{-2} . For the 1- μm -thick Mg-doped GaN films, typical full width at half maximum values of X-ray rocking curves for 0002 and $10\bar{1}2$ diffraction were 320 and 360 arcsec, respectively. These values were almost independent of the Mg doping concentration. For Hall-effect measurements, the samples were processed into the Van der Pauw structure with a clover-leaf design using photolithography and inductively coupled plasma (ICP)-RIE. Pd/Au (30 nm/100 nm) was used as an ohmic contact, and its typical resistance was $5 \times 10^{-4} \Omega \text{ cm}^2$. No high-temperature thermal-activation process was performed for any sample used in this study. A temperature-dependent Hall-effect measurement system included MMR Joule-Thomson variable temperature sample holders, a 0.5 T fixed magnet, and ADVANTEST electronic equipment. Analytical protocol basically followed ASTM standard F76¹³ with a Hall scattering factor of unity.

Figure 1 shows a SIMS depth profile for Mg and H in a step-graded Mg-doped GaN. A stepwise, controlled Mg-doping profile and clear interfaces between Mg-doped GaN and nondoped GaN are observed. These data indicate that Mg diffusion was sufficiently suppressed during growth. Moreover, this result indicates that the memory effect for Mg doping, which is problematic for the formation of abrupt doping profiles in the case of MOCVD growth,¹⁴ was negligible during PSD growth. This advantage can be attributed to the lower growth temperature of PSD compared

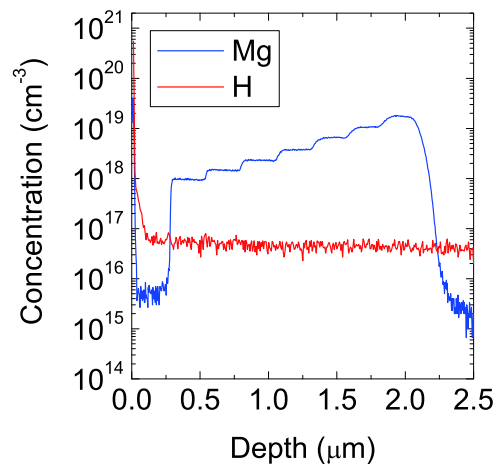


FIG. 1. SIMS depth profile of Mg in Mg-doped GaN grown by PSD. Mg doping concentration dependence of residual hydrogen concentration in Mg doped GaN estimated by SIMS. Blue and red lines indicate Mg and hydrogen concentration profiles, respectively. The detection limits for Mg and hydrogen are 4×10^{15} and $5 \times 10^{16} \text{ cm}^{-3}$, respectively.

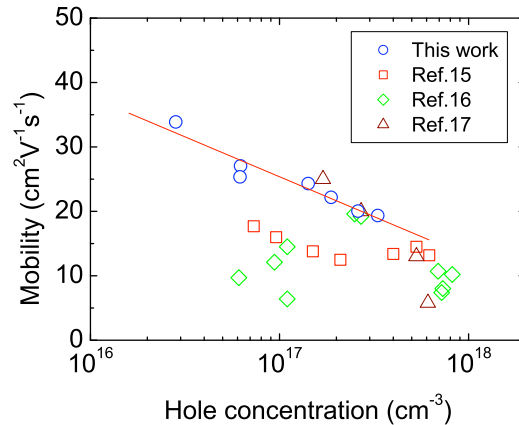


FIG. 2. The relationship between hole concentration and hole mobility in Mg-doped GaN grown by PSD at RT. Open circles and squares represent our experimental data and previously reported MOCVD data, respectively (red,¹⁵ green,¹⁶ brown¹⁷).

to MOCVD. Figure 1 also shows how the residual hydrogen concentration depends on the Mg doping concentration. In the case of MOCVD growth, hydrogen atoms are incorporated into GaN simultaneously with Mg; thus, the hydrogen concentration is on the same order as the Mg concentration.⁷ In contrast to MOCVD growth, the hydrogen concentration during PSD growth remained below the detection limit of $5 \times 10^{16} \text{ cm}^{-3}$ even at high Mg concentration. We also found that both residual oxygen and silicon concentrations were below the detection limit of $1 \times 10^{16} \text{ cm}^{-3}$; that is, they were significantly low compared to the Mg concentration in this study. These results clearly demonstrate the advantage of the low-temperature PSD process for the preparation of high-purity p-type GaN for abrupt p-n junctions.

Next, we investigated the electrical properties of Mg-doped GaN with low hydrogen concentrations using Hall-effect measurements at room temperature (RT). All of the as-grown Mg-doped GaN films showed clear p-type conductivity at RT without thermal annealing. This is consistent with the low residual hydrogen concentration confirmed by SIMS measurements. Figure 2 shows the relationship between the experimentally determined hole concentration and hole mobility for the p-type GaN films grown by PSD. The reported values for p-type GaN on sapphire grown by MOCVD are also plotted in Figure 2.¹⁵⁻¹⁷ The hole mobility of our samples increased monotonically with decreasing hole concentration. For lightly Mg-doped GaN films ($[\text{Mg}] = 7.9 \times 10^{17} \text{ cm}^{-3}$), the hole mobility reached $34 \text{ cm}^2 \text{ V}^{-1} \text{ s}^{-1}$ at RT. The hole mobilities of our samples were as high as or higher than those obtained via MOCVD, implying that our samples were less compensated than the MOCVD samples. This is likely attributed to the reduction in the concentrations of residual hydrogen and/or other donors in the p-type GaN films grown by PSD. Recently, several MBE groups have also grown Mg-doped GaN with excellent electrical properties such as a high hole mobility of around $30 \text{ cm}^2 \text{ V}^{-1} \text{ s}^{-1}$ at RT¹⁸ and much higher hole concentration over 10^{19} cm^{-3} at RT.¹⁹ These results indicate that physical vapor deposition techniques such as MBE or PSD are quite attractive for the growth of high-quality p-type GaN.

To elucidate the hole transport properties of p-type PSD GaN, we also performed temperature-dependent Hall-effect measurements. Figure 3 shows the temperature dependence of hole mobility for our p-type GaN films. At temperatures above 500 K, the temperature dependences of all samples were similar regardless of the Mg doping concentration, likely because the hole mobility was limited primarily by lattice scattering.²⁰ For relatively heavily Mg-doped GaN ($[\text{Mg}] > 4.1 \times 10^{19} \text{ cm}^{-3}$), the mobility monotonically increased with decreasing temperature and reached a peak value of around $30 \text{ cm}^2 \text{ V}^{-1} \text{ s}^{-1}$ at 200 K. This peak mobility was probably limited by the neutral impurity scattering. In this low temperature range, you can also see clear increase in the hole mobility with decreasing Mg concentration because of the reduced scattering rate of neutral impurities. For lightly Mg-doped GaN ($[\text{Mg}] = 7.9 \times 10^{17} \text{ cm}^{-3}$), the hole mobility reached $62 \text{ cm}^2 \text{ V}^{-1} \text{ s}^{-1}$ at 175 K, which is as high as that of p-type GaN fabricated by MOCVD.^{21,22} These

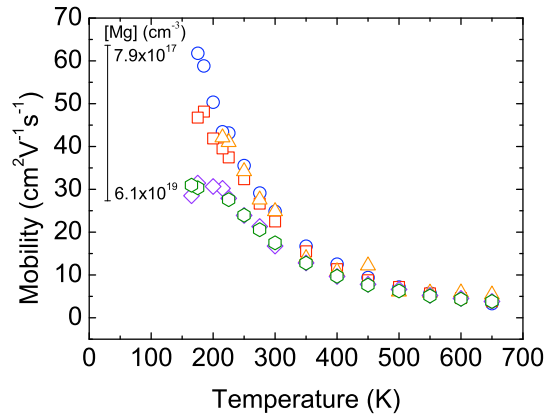


FIG. 3. Temperature dependence of hole mobility in PSD-grown Mg-doped GaN with $[Mg]$ ranging from 7.9×10^{17} to $6.1 \times 10^{19} \text{ cm}^{-3}$.

excellent electrical properties of p-type GaN can be attributed to a reduction in the residual donor concentration.

To estimate the activation energy E_A of Mg acceptor, we investigated the temperature dependence of hole concentration in p-type GaN formed by PSD. Figure 4(a) shows the temperature dependence of hole concentration between 175 and 650 K for different Mg concentrations. The fitting curves were obtained under charge-neutral conditions in a nondegenerate p-type semiconductor using the following equation:

$$\frac{p(p + N_D)}{N_A - N_D - p} = \frac{N_V}{g} \exp\left(-\frac{E_A}{k_B T}\right), \quad (1)$$

where p is hole concentration, g is acceptor degeneracy factor ($=4$), k_B is Boltzmann's constant, T is temperature, and N_V is the effective density of states in the valence band. To calculate N_V , we used the hole effective mass of 2.2.²³ The experimental data were well fitted by Eq. (1), and the acceptor concentration N_A obtained through fitting was in good agreement with the Mg concentration determined by SIMS. However, the compensating donor concentration N_D obtained by this fitting was much higher than that estimated by SIMS; for example, the fitted value of N_D for p-type GaN with $[Mg] = 7.9 \times 10^{17} \text{ cm}^{-3}$ was $2.5 \times 10^{17} \text{ cm}^{-3}$, whereas the total concentration of H, O, and Si atoms in the film determined by SIMS was much lower. This large discrepancy in donor concentration may be explained by the incorporation of intrinsic defects such as nitrogen vacancies and/or their complexes with Mg. To reduce these intrinsic defects, the growth conditions should be

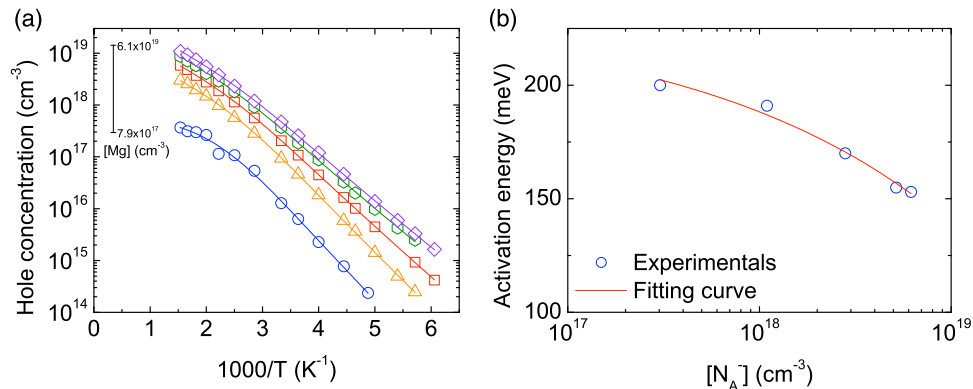


FIG. 4. (a) Arrhenius plots of hole concentration and (b) activation energy as a function of ionized acceptor concentration and the fitting curve for PSD-grown Mg-doped GaN with $[N_A]$ ranging from 7.9×10^{17} to $6.1 \times 10^{19} \text{ cm}^{-3}$.

further optimized. According to recent progresses in MBE growth of p-type GaN, reduction in the growth temperature makes it possible to suppress the incorporation of such intrinsic defects due to their higher formation energy at lower temperatures, which is quite instructive for our case.²⁴ The E_A value of Mg acceptor for each sample is plotted in Fig. 4(b) as a function of an ionized acceptor concentration N_A^- . E_A decreased in proportion to $(N_A^-)^{1/3}$ due to the Coulomb interaction between ionized acceptors and the screening of the Coulomb potential by free carriers. The inherent depth of the Mg acceptor level was estimated to be 231 meV by curve fitting in Fig. 4(a). For the fitting, we used a dielectric constant of 9.5 for GaN. The obtained value (231 meV) was close to the recently reported value of 235 meV.²¹ These values may be more reliable because they were obtained from the data of lightly Mg-doped samples.

In summary, we prepared Mg-doped GaN films using PSD and investigated the hole transport properties. SIMS measurements revealed that the concentration of residual hydrogen was below the detection limit of $5 \times 10^{16} \text{ cm}^{-3}$. Thanks to the remarkably low hydrogen concentration, all the Mg-doped GaN samples showed p-type conductivity without thermal annealing. We confirmed that the Mg profile can be precisely controlled, and the problematic memory effect or dopant diffusion was not observed. Lightly Mg-doped samples ($[\text{Mg}] = 7.9 \times 10^{17} \text{ cm}^{-3}$) showed high hole mobilities of 34 and $62 \text{ cm}^2 \text{ V}^{-1} \text{ s}^{-1}$ at RT and 175 K, respectively. The depth of the Mg acceptor level was estimated to be 231 meV. The excellent electrical properties can be attributed to the reduction in the concentration of residual donors such as hydrogen, oxygen, and silicon. These results indicate that PSD is a powerful tool for the fabrication of vertical power devices.

- ¹ Y. Saitoh, K. Sumiyoshi, M. Okada, T. Horii, T. Miyazaki, H. Shiomii, M. Ueno, K. Katayama, M. Kiyama, and T. Nakamura, *Appl. Phys. Express* **3**, 081001 (2010).
- ² Y. Cao, R. Chu, R. Li, M. Chen, R. Chang, and B. Hughes, *Appl. Phys. Lett.* **108**, 062103 (2016).
- ³ Z. Hu, K. Nomoto, B. Song, M. Zhu, M. Qi, M. Pan, X. Gao, V. Protasenko, D. Jena, and H. G. Xing, *Appl. Phys. Lett.* **107**, 243501 (2015).
- ⁴ I. C. Kizilyalli, A. P. Edwards, O. Aktas, T. Prunty, and D. Bour, *IEEE Trans. Electron Devices* **62**, 414 (2015).
- ⁵ T. Oka, T. Ina, Y. Ueno, and J. Nishii, *Appl. Phys. Express* **8**, 054101 (2015).
- ⁶ S. Nakamura, T. Mukai, M. Senoh, and N. Iwasa, *Jpn. J. Appl. Phys., Part 2* **31**, L139 (1992).
- ⁷ A. Castiglia, J. F. Carlin, and N. Grandjean, *Appl. Phys. Lett.* **98**, 213505 (2011).
- ⁸ K. Orita, M. Meneghini, H. Ohno, N. Trivellin, N. Ikedo, S. Takigawa, M. Yuri, T. Tanaka, E. Zanoni, and G. Meneghesso, *IEEE J. Quantum Electron.* **48**, 1169 (2012).
- ⁹ K. Ueno, E. Kishikawa, S. Inoue, J. Ohta, H. Fujioka, M. Oshima, and H. Fukuyama, *Phys. Status Solidi RRL* **8**, 256 (2013).
- ¹⁰ E. Nakamura, K. Ueno, J. Ohta, H. Fujioka, and M. Oshima, *Appl. Phys. Lett.* **104**, 051121 (2014).
- ¹¹ J. W. Shon, J. Ohta, K. Ueno, A. Kobayashi, and H. Fujioka, *Sci. Rep.* **4**, 5325 (2014).
- ¹² T. Watanabe, J. Ohta, T. Kondo, M. Ohashi, K. Ueno, A. Kobayashi, and H. Fujioka, *Appl. Phys. Lett.* **104**, 182111 (2014).
- ¹³ ASTM International, *ASTM Standard F76, Test Methods for Measuring Resistivity and Hall Coefficient and Determining Hall Mobility in Single-Crystal Semiconductors* (ASTM International, West Conshohocken, PA, 2011).
- ¹⁴ Y. Ohba and A. Hatano, *J. Cryst. Growth* **145**, 214 (1994).
- ¹⁵ M. G. Cheong, K. S. Kim, C. S. Kim, R. J. Choi, H. S. Yoon, N. W. Namgung, E. K. Suh, and H. J. Lee, *Appl. Phys. Lett.* **80**, 1001 (2002).
- ¹⁶ P. Kozodoy, S. Keller, S. P. DenBaars, and U. K. Mishra, *J. Cryst. Growth* **195**, 265 (1998).
- ¹⁷ P. Kozodoy, S. P. DenBaars, and U. K. Mishra, *J. Appl. Phys.* **87**, 770 (2000).
- ¹⁸ H. Okumura, D. Martin, M. Malinverni, and N. Grandjean, *Appl. Phys. Lett.* **108**, 072102 (2016).
- ¹⁹ S. D. Burnham, G. NamKoong, D. C. Look, B. Clafin, and W. A. Doolittle, *J. Appl. Phys.* **104**, 024902 (2008).
- ²⁰ K. S. Kim, M. G. Cheong, C. H. Hong, G. M. Yang, K. Y. Lim, E. K. Suh, and H. J. Lee, *Appl. Phys. Lett.* **76**, 1149 (2000).
- ²¹ M. Horita, S. Takashima, R. Tanaka, H. Matsuyama, K. Ueno, M. Edo, and J. Suda, *Jpn. J. Appl. Phys., Part 1* **55**, 05FH03 (2016).
- ²² P. Kozodoy, H. Xing, S. P. DenBaars, and U. K. Mishra, *J. Appl. Phys.* **87**, 1832 (2000).
- ²³ J. S. Im, A. Moritz, F. Steuber, V. Härle, F. Scholz, and A. Hangleiter, *Appl. Phys. Lett.* **70**, 631 (1997).
- ²⁴ B. P. Gunning, C. A. M. Fabien, J. J. Merola, E. A. Clinton, W. A. Doolittle, S. Wang, A. M. Ficher, and F. A. Ponce, *J. Appl. Phys.* **117**, 045710 (2015).